

Variational Nonlinear System Identification

Jarrad Courts^{*1}, Adrian Wills^{†1}, Thomas B. Schön^{‡, §2}, and Brett Ninness^{¶1}

¹*University of Newcastle, School of Engineering, Australia*

²*Department of Information Technology, Uppsala University, Uppsala, Sweden*

December 10, 2020

Abstract

This paper considers parameter estimation for nonlinear state-space models, which is an important but challenging problem. We address this challenge by employing a variational inference (VI) approach, which is a principled method that has deep connections to maximum likelihood estimation. This VI approach ultimately provides estimates of the model as solutions to an optimisation problem, which is deterministic, tractable and can be solved using standard optimisation tools. A specialisation of this approach for systems with additive Gaussian noise is also detailed. The proposed method is examined numerically on a range of simulation and real examples with a focus on robustness to parameter initialisations; we additionally perform favourable comparisons against state-of-the-art alternatives.

1 Introduction

The problem of system identification is long-standing and has significant practical applications. As such, there exists a large body of related literature across many different fields and classes of systems [23, 16]. This paper is directed towards identification of the widely applicable, and very flexible, class of systems described by nonlinear state-space models. It is well recognised that the problem of system identification of nonlinear state-space models is both important and difficult [26, 31].

The problem of system identification for nonlinear state-space models consists of making use of the measurements $\mathbf{y} \triangleq y_{1:T} \triangleq \{y_1, \dots, y_T\}$ to compute an estimate of the model parameters $\theta \in \mathcal{R}^{n_\theta}$ for the following model structure

$$x_{k+1} \sim p_\theta(x_{k+1} | x_k), \quad (1a)$$

$$y_k \sim p_\theta(y_k | x_k), \quad (1b)$$

where $x_k \in \mathcal{R}^{n_x}$, $y_k \in \mathcal{R}^{n_y}$ and p denotes a probability density function.

This estimate can be defined in several different ways depending on various user choices. Relevant to the current work is the underlying assumptions made regarding the unknown parameters. Along this line, if the uncertainty concerning the parameters is modelled by treating θ as a random variable, then the so-called Bayesian methods are appropriate, where the goal is to compute an estimate of the posterior distribution for θ via

$$p(\theta | \mathbf{y}) = \frac{p(\mathbf{y} | \theta) p(\theta)}{p(\mathbf{y})}. \quad (2)$$

Alternatively, if the parameters are treated as deterministic, but unknown, then point estimates of θ can be provided by the maximum likelihood (ML) approach

$$\theta_{\text{ML}} = \arg \max_{\theta} \log p(\mathbf{y} | \theta). \quad (3)$$

^{*}jarrad.courts@uon.edu.au

[†]Adrian.Wills@newcastle.edu.au

[‡]thomas.schon@it.uu.se

[§]This research was financially supported by the Swedish Foundation for Strategic Research (SSF) via the project *ASSEMBLE* (contract number: RIT15-0012) and by the Swedish Research Council via the projects *Learning flexible models for nonlinear dynamics* (contract number: 2017-03807) and *NewLEADS - New Directions in Learning Dynamical Systems* (contract number: 621-2016-06079) and by the project *A14Research* at Uppsala University.

[¶]brett.ninness@newcastle.edu.au

A maximum likelihood based approach of estimating parameters has desirable statistical properties and many system identification approaches aim to obtain the ML estimate of θ given by θ_{ML} [36, 23, 31].

To obtain θ_{ML} via (3) requires calculation, followed by optimisation of the likelihood function $p(\mathbf{y} | \theta)$. By repeated application of conditional probability, this is given by

$$p(\mathbf{y} | \theta) = p_{\theta}(y_1) \prod_{k=2}^T p_{\theta}(y_k | y_{1:k-1}), \quad (4)$$

where, due to the Markovian nature of state-space models, the output prediction density can be expressed as

$$p(y_k | y_{1:k-1}) = \int p_{\theta}(y_k | x_k) p_{\theta}(x_k | y_{1:k-1}) dx_k,$$

and where the state prediction density is given by

$$p_{\theta}(x_{k+1} | y_{1:k}) = \int \frac{p_{\theta}(y_k | x_k) p_{\theta}(x_k | y_{1:k-1})}{p(y_k | y_{1:k-1})} p_{\theta}(x_{k+1} | x_k) dx_k.$$

Together these equations allow the likelihood to be recursively calculated [35, 36]. Unfortunately, the use of these equations to evaluate, and then optimise, $p(\mathbf{y} | \theta)$ remains generally intractable due to the integrals and arbitrary probability distributions involved.

Despite this, “direct” gradient-based approaches to ML system identification exists which utilise *approximations* of both the intractable integrals and filtered/predicted probability distributions required [20]. This approach, however, can be difficult to implement. In particular, the resulting optimisation problem typically possess many local minima making this approach not robust with respect to the initial parameter estimate which can be a significant problem [25, 24, 31].

Alternatively, expectation maximisation (EM) [9] can be used. Contrary to “direct” gradient-based approaches, EM does not attempt to directly maximise $p(\mathbf{y} | \theta)$. Rather the expectation step (E-step), based on state smoothing, forms a function which is a lower bound of the likelihood, this function is then maximised (M-step); generally, this maximisation possesses no closed form. The critical property of EM is that each iteration provably produces parameter estimates which monotonically increase the likelihood [5].

Similar to the direct approach, this guarantee requires exact evaluation of the intractable integrals mentioned above. As such, EM cannot exactly be performed; instead *approximations* must be used. A result of this is that guarantees regarding the monotonic increase in likelihood are no longer applicable. Despite this, EM performed using various approximations [36, 6, 11, 19] has been demonstrated as a robust approach to performing ML system identification.

In this paper, the primary contribution is presenting a variational inference (VI) [17, 3] based approach to system identification. This approach is related to EM-based methods and *exactly* provides parameter estimates which *approximate* θ_{ML} . Differing from EM-based approaches, the approach taken allows for the all approximations regarding intractable integrals and the form of probability distributions to be explicitly acknowledged. The result of this is a single, tractable, optimisation problem, which simultaneously estimates both model parameters and an assumed density estimate of the smoothed state distribution.

A common approach used in VI [3] is to assume a *mean-field variational family* [2] in order to simplify calculations. As will be detailed in this paper, this and related assumptions are not particularly well suited to state-space dynamic systems. In contrast, this paper uses an alternative approach where the VI problem is formulated as *constrained* problem. The primary benefit of this approach is that it simplifies the required calculations without introducing unnecessary and restrictive assumptions. Importantly, we detail this optimisation problem formulation and show how exact first- and second-order derivatives can be calculated and used in solving this problem. We further specialise this presentation for the important class of system models with additive Gaussian noise.

The remainder of this paper is organised as follows; Section 2 examines the application of variational inference in the context of the identification of nonlinear state-space models and the relationship to expectation maximisation. Section 3 details the specific assumed density form considered and approximation required to result in a tractable optimisation problem along with the additive Gaussian noise specialisation. This is followed by implementation details in Section 4 and several numerical examples in Section 5. Section 6 concludes the paper.

2 Variational Nonlinear System Identification

In this section, the use of variational inference applied to nonlinear state space systems will be presented in Section 2.1. The relationship between variational inference and expectation maximisation is then examined in Section 2.2.

2.1 Variational Inference

Variational inference is a widely used method to approximate, potentially intractable, posterior distributions with a parametric density of an assumed form. This is achieved through optimisation of a likelihood lower bound [3].

Using conditional probability, this lower bound can be found by expressing the log-likelihood, $\log p_\theta(\mathbf{y})$, as

$$\log p_\theta(\mathbf{y}) = \log p_\theta(\mathbf{x}, \mathbf{y}) - p_\theta(\mathbf{x} | \mathbf{y}), \quad (5)$$

where $\mathbf{x} \triangleq x_{1:T+1} \triangleq \{x_1, \dots, x_{T+1}\}$. As $p_\theta(\mathbf{x} | \mathbf{y})$ is intractable it is approximated using an assumed density, parameterised by β , and denoted as $q_\beta(\mathbf{x})$. Through addition and subtraction of $\log q_\beta(\mathbf{x})$ to the right-hand side of (5) this leads to

$$\log p_\theta(\mathbf{y}) = \log \frac{p_\theta(\mathbf{x}, \mathbf{y})}{q_\beta(\mathbf{x})} + \log \frac{q_\beta(\mathbf{x})}{p_\theta(\mathbf{x} | \mathbf{y})}. \quad (6)$$

Due to the independence of $\log p_\theta(\mathbf{y})$ from \mathbf{x} , the log-likelihood can alternatively be given by

$$\log p_\theta(\mathbf{y}) = \int q_\beta(\mathbf{x}) \log p_\theta(\mathbf{y}) d\mathbf{x}. \quad (7)$$

Substituting (6) into the right-hand side of (7) results in

$$\begin{aligned} \log p_\theta(\mathbf{y}) &= \int q_\beta(\mathbf{x}) \log \frac{p_\theta(\mathbf{x}, \mathbf{y})}{q_\beta(\mathbf{x})} d\mathbf{x} \\ &\quad + \int q_\beta(\mathbf{x}) \log \frac{q_\beta(\mathbf{x})}{p_\theta(\mathbf{x} | \mathbf{y})} d\mathbf{x}, \end{aligned} \quad (8)$$

which will be expressed as

$$\log p_\theta(\mathbf{y}) = \mathcal{L}(\beta, \theta) + \text{KL}[q_\beta(\mathbf{x}) || p_\theta(\mathbf{x} | \mathbf{y})]. \quad (9)$$

Here, $\text{KL}[q_\beta(\mathbf{x}) || p_\theta(\mathbf{x} | \mathbf{y})]$ is the Kullback-Leiber (KL) [21] divergence of $p_\theta(\mathbf{x} | \mathbf{y})$ from $q_\beta(\mathbf{x})$ and

$$\mathcal{L}(\beta, \theta) = \int q_\beta(\mathbf{x}) \log \frac{p_\theta(\mathbf{x}, \mathbf{y})}{q_\beta(\mathbf{x})} d\mathbf{x}. \quad (10)$$

Due to the non-negativity of any KL divergence, equation (9) implies that

$$\log p_\theta(\mathbf{y}) \geq \mathcal{L}(\beta, \theta). \quad (11)$$

Therefore $\mathcal{L}(\beta, \theta)$ is a lower bound to the log-likelihood $\log p_\theta(\mathbf{y})$ and it is also known as the evidence lower bound (ELBO) and (negative) variational free energy [3, 38]. The tightness of this bound, given by $\text{KL}[q_\beta(\mathbf{x}) || p_\theta(\mathbf{x} | \mathbf{y})]$, depends upon two elements, the assumed form of $q_\beta(\mathbf{x})$ compared to $p_\theta(\mathbf{x} | \mathbf{y})$, and the value of β .

The approach to system identification proposed in this paper is to simultaneously find values for β and θ , denoted respectively as β^* and θ^* , that maximise $\mathcal{L}(\beta, \theta)$ via

$$\beta^*, \theta^* = \arg \max_{\beta, \theta} \mathcal{L}(\beta, \theta), \quad (12)$$

for a given assumed density form. The parameter estimate is then given by θ^* . Generally, this will not be the ML parameter estimate, i.e. $\theta^* \neq \theta_{\text{ML}}$. In the situation where the assumed density $q_\beta(\mathbf{x})$ has sufficient flexibility to allow that $\text{KL}[q_{\beta^*}(\mathbf{x}) || p_\theta(\mathbf{x} | \mathbf{y})] = 0$ for some β^* , it follows from (9) that

$$\log p_\theta(\mathbf{y}) = \mathcal{L}(\beta^*, \theta). \quad (13)$$

Therefore, $\theta^* = \theta_{\text{ML}}$ will hold in this case since no approximations have been introduced. More generally, it is hoped that choosing a suitable parametric form for $q_\beta(\mathbf{x})$ such that $\text{KL}[q_{\beta^*}(\mathbf{x}) \parallel p_\theta(\mathbf{x} \mid \mathbf{y})]$ is small will provide a tight lower bound on $\log p_\theta(\mathbf{y})$, and hence $\theta^* \approx \theta_{\text{ML}}$.

The primary benefit, then, of the VI approach stems from the flexibility in choosing $q_\beta(\mathbf{x})$ so that (12) is both computationally tractable and amenable to standard optimisation tools. Countering this benefit is that the variational inference approach is aiming to solve a slightly different problem compared to the ML problem of (3). The following section highlights the connection, and difference between an EM approach for solving the ML problem (3) and the proposed VI approach leading to (12).

2.2 Relationship to Expectation-Maximisation

There are close connections between solutions based on EM and VI, see e.g. [30] and [37] for concrete examples. In this section some of these relationships, in the context of identification of nonlinear state space models, will be examined. This is to allow for a more intuitive understanding of the relationship and differences between the proposed system identification approach and established EM system identification methods.

The EM approach consists of iterating between the following steps:

1. E-Step: Form $\mathcal{Q}(\theta, \theta_k)$,
2. M-Step: $\theta_{k+1} = \arg \max_\theta \mathcal{Q}(\theta, \theta_k)$,

where

$$\mathcal{Q}(\theta, \theta_k) = \int p_{\theta_k}(\mathbf{x} \mid \mathbf{y}) \log p_\theta(\mathbf{x}, \mathbf{y}) d\mathbf{x},$$

and produces parameters estimates θ_k that monotonically increase $\log p_{\theta_k}(\mathbf{y})$ [5]. It is important to notice that central to each E-step is obtaining the smoothed distribution $p_{\theta_k}(\mathbf{x} \mid \mathbf{y})$.

The following Lemma reveals that the E and M steps can be viewed as block-ascent of the VI cost $\mathcal{L}(\beta, \theta)$ over β and then θ , respectively. This requires an assumption on $q_\beta(\mathbf{x})$, which essentially means that it is possible to match the smoothed density $p_{\theta_k}(\mathbf{x} \mid \mathbf{y})$ using KL divergence.

Lemma 1. *Assume that it is possible to choose $q_\beta(\mathbf{x})$ such that*

$$\text{KL}[q_\beta(\mathbf{x}) \parallel p_{\theta_k}(\mathbf{x} \mid \mathbf{y})] = 0. \quad (14)$$

Then the EM iterations can be expressed as

1. E-Step: $\beta^* = \arg \max_\beta \mathcal{L}(\beta, \theta_k)$,
2. M-Step: $\theta_{k+1} = \arg \max_\theta \mathcal{L}(\beta^*, \theta)$.

Proof. Under assumption (14), $\text{KL}[q_\beta(\mathbf{x}) \parallel p_{\theta_k}(\mathbf{x} \mid \mathbf{y})]$ has a global minimum value of zero, which is achieved for any $\beta^* = \arg \min_\beta \text{KL}[q_\beta(\mathbf{x}) \parallel p_{\theta_k}(\mathbf{x} \mid \mathbf{y})]$. Utilising (9) it holds that $\text{KL}[q_\beta(\mathbf{x}) \parallel p_{\theta_k}(\mathbf{x} \mid \mathbf{y})] = \log p_{\theta_k}(\mathbf{y}) - \mathcal{L}(\beta, \theta_k)$, and notice that $\log p_{\theta_k}(\mathbf{y})$ is constant over β , therefore

$$\begin{aligned} \beta^* &= \arg \min_\beta \text{KL}[q_\beta(\mathbf{x}) \parallel p_{\theta_k}(\mathbf{x} \mid \mathbf{y})] \\ &= \arg \min_\beta \log p_{\theta_k}(\mathbf{y}) - \mathcal{L}(\beta, \theta_k) \\ &= \arg \max_\beta \mathcal{L}(\beta, \theta_k). \end{aligned}$$

It follows immediately that $\text{KL}[q_{\beta^*}(\mathbf{x}) \parallel p_{\theta_k}(\mathbf{x} \mid \mathbf{y})] = 0$, hence the E-step equivalence. The M-step can be expressed as

$$\begin{aligned} \theta_{k+1} &= \arg \max_\theta \mathcal{Q}(\theta, \theta_k) \\ &= \arg \max_\theta \int p_{\theta_k}(\mathbf{x} \mid \mathbf{y}) \log p_\theta(\mathbf{x}, \mathbf{y}) d\mathbf{x} \\ &= \arg \max_\theta \int q_{\beta^*}(\mathbf{x}) \log p_\theta(\mathbf{x}, \mathbf{y}) d\mathbf{x}. \end{aligned}$$

Further, as $\int q_{\beta^*}(\mathbf{x}) \log q_{\beta^*}(\mathbf{x}) d\mathbf{x}$ is independent of θ ,

$$\begin{aligned}\theta_{k+1} &= \arg \max_{\theta} \left(\int q_{\beta^*}(\mathbf{x}) \log p_{\theta}(\mathbf{x}, \mathbf{y}) d\mathbf{x} \right. \\ &\quad \left. - \int q_{\beta^*}(\mathbf{x}) \log q_{\beta^*}(\mathbf{x}) d\mathbf{x} \right) \\ &= \arg \max_{\theta} \int q_{\beta^*}(\mathbf{x}) \log \frac{p_{\theta}(\mathbf{x}, \mathbf{y})}{q_{\beta^*}(\mathbf{x})} d\mathbf{x} \\ &= \arg \max_{\theta} \mathcal{L}(\beta^*, \theta).\end{aligned}$$

□

□

Presenting EM in this form highlights that both EM and VI make progress by optimising a common lower bound (see also [37]).

It is, however, important to recognise that, generally, it is not possible to select a *tractable* $q_{\beta}(\mathbf{x})$ such that $\text{KL}[q_{\beta}(\mathbf{x}) \parallel p_{\theta_k}(\mathbf{x} \mid \mathbf{y})] = 0$. Similarly, exactly computing the expectations with respect to the smoothed distribution $p_{\theta_k}(\mathbf{x} \mid \mathbf{y})$ is generally not possible for nonlinear state-space models. As such, exactly performing EM on nonlinear state-space models is, generally, intractable.

Despite this, the EM approach to system identification has motivated several successful approximate EM methods. These utilise a variety of approximations for $p_{\theta_k}(\mathbf{x} \mid \mathbf{y})$ and the required expectations; these include particle smoothing based EM [36] and unscented Rauch-Tung-Striebel smoothing [34] based EM [11] among others [6, 19]. The introduction of these approximations, however, comes at the cost of guaranteed monotonic behaviour of EM and the approximations are not necessarily consistent between the E-step and the M-step.

Alternatively to approximating $p_{\theta_k}(\mathbf{x} \mid \mathbf{y})$, it is possible to relax the restriction that $\text{KL}[q_{\beta}(\mathbf{x}) \parallel p_{\theta_k}(\mathbf{x} \mid \mathbf{y})] = 0$ must occur. This allows for the selection of a convenient form for $q_{\beta}(\mathbf{x})$ to be utilised within the EM framework and is known as variational EM [3, 37]. This differs from approximate EM methods which, generally, allow for *any* arbitrary approximation of $p_{\theta_k}(\mathbf{x} \mid \mathbf{y})$. Variational EM, however, enforces that $p_{\theta_k}(\mathbf{x} \mid \mathbf{y})$ is approximated by $q_{\beta^*}(\mathbf{x})$, the distribution of the assumed form which minimises $\text{KL}[q_{\beta}(\mathbf{x}) \parallel p_{\theta_k}(\mathbf{x} \mid \mathbf{y})]$. This more consistent application of approximations ensures a sequence of θ_k that monotonically increase the log-likelihood.

The variational EM approach is closely related to block coordinate descent of the proposed identification method, (12). We therefore anticipate that the proposed approach to system identification should possess an improved rate of convergence compared to variational EM without introducing any further assumptions or approximations. This is expected because optimisation over all variables generally converge more rapidly than coordinate descent counterparts, particularly when the variables are strongly coupled.

3 Assumed Gaussian Distribution and Tractable Approximation

While (12) avoids distributions that are intractable due to their arbitrary form, the problem remains computationally intractable for two reasons. Firstly, as per [35], any calculation involving the full posterior distribution $q_{\beta}(\mathbf{x})$ will become computationally intractable simply due to the large dimension of \mathbf{x} . Secondly, calculation of $\mathcal{L}(\beta, \theta)$ involves intractable nonlinear integrals, regardless of how manageable $q_{\beta}(\mathbf{x})$ is.

In this section, we first show that the full distribution $q_{\beta}(\mathbf{x})$ is not required, rather only the pairwise joints given by $q_{\beta}(x_k, x_{k+1})$ are needed. To a large extent, this deals with the first concern mentioned above. To address the second concern, we propose to employ a multivariate Gaussian distribution for $q_{\beta}(x_k, x_{k+1})$, which results in a tractable and deterministic optimisation problem for the VI approach.

3.1 Pairwise Joints

To tractably utilise the approach given by (12) it is required to express $\mathcal{L}(\beta, \theta)$ as a function of each $q_{\beta}(x_k, x_{k+1})$ rather than $q_{\beta}(\mathbf{x})$.

Due to the Markovian nature of state space models and conditional probability, similar to [36, 6, 35, 38, 8] among

others, we can write

$$\begin{aligned}\mathcal{L}(\beta, \theta) &= \int q_\beta(\mathbf{x}) \log \frac{p_\theta(\mathbf{x}, \mathbf{y})}{q_\beta(\mathbf{x})} d\mathbf{x} \\ &= I_1(\beta) + I_2(\beta, \theta) + I_3(\beta, \theta) - I_4(\beta),\end{aligned}$$

where

$$\begin{aligned}I_1(\beta) &= \int q_\beta(x_1) \log p(x_1) dx_1, \\ I_2(\beta, \theta) &= \sum_{k=1}^T \int q_\beta(x_{k:k+1}) \log p_\theta(x_{k+1} | x_k) dx_{k:k+1}, \\ I_3(\beta, \theta) &= \sum_{k=1}^T \int q_\beta(x_k) \log p_\theta(y_k | x_k) dx_k, \\ I_4(\beta) &= \sum_{k=1}^T \int q_\beta(x_{k:k+1}) \log q_\beta(x_{k:k+1}) dx_{k:k+1} \\ &\quad - \sum_{k=2}^T \int q_\beta(x_k) \log q_\beta(x_k) dx_k.\end{aligned}$$

As desired this expresses $\mathcal{L}(\beta, \theta)$ in terms of each $q_\beta(x_k, x_{k+1})$ rather than $q_\beta(\mathbf{x})$. This greatly reduces the size of the space that we are integrating over. Nevertheless, in order to provide a practical algorithm, it is essential that these integrals can be computed, or accurately approximated. This is discussed in the next section.

3.2 Assumed Gaussian Distribution

As detailed above, the given VI approach to system identification relies upon the provision of an assumed parametric form for each pairwise joint distribution, $q_\beta(x_k, x_{k+1})$. When selecting this form, two goals should be kept in mind. Firstly, $q_\beta(x_k, x_{k+1})$ should be selected such that it can accurately approximate the intractable $p_\theta(x_k, x_{k+1} | \mathbf{y})$. Secondly, $q_\beta(x_k, x_{k+1})$ should be selected such that the required expectations over each pairwise joint can be readily and accurately approximated. Satisfying these aims will result in an optimisation problem that can be solved using standard optimisation tools.

Towards achieving these goals, in this paper we have selected a multivariate Gaussian to represent each pairwise joint distribution. Using Gaussian assumptions for the state distribution is a widely performed and effective approximation [35]. Equally, if not perhaps more importantly, this assumption allows for a tractable optimisation problem with exact first- and second-order derivatives to be formed using readily available integral approximations. The resulting, constrained, optimisation problem is in a form that can be directly handled by standard nonlinear programming routines.

To this end, each joint normally distributed assumed density will be parameterised as

$$q_{\beta_k}(x_k, x_{k+1}) = \mathcal{N}\left(\begin{bmatrix} x_k \\ x_{k+1} \end{bmatrix}; \begin{bmatrix} \mu_k \\ \bar{\mu}_k \end{bmatrix}, P_k^{\frac{1}{2}} P_k^{\frac{1}{2}}\right), \quad (15)$$

where $\mu_k \in \mathcal{R}^{n_x \times 1}$, $\bar{\mu}_k \in \mathcal{R}^{n_x \times 1}$, and $P_k^{\frac{1}{2}} \in \mathcal{R}^{2n_x \times 2n_x}$ describe the joint state distribution and

$$P_k^{\frac{1}{2}} = \begin{bmatrix} A_k & B_k \\ 0 & C_k \end{bmatrix}, \quad (16)$$

where $A_k, B_k, C_k \in \mathcal{R}^{n_x \times n_x}$ and A_k, C_k are upper triangular. The parameter β_k is now given as

$$\beta_k = \{\mu_k, \bar{\mu}_k, A_k, B_k, C_k\}, \quad (17)$$

and related to β via

$$\beta = \{\beta_1, \beta_2, \dots, \beta_T\}. \quad (18)$$

Algorithm 1 General identification approach

Input: Measurements $y_{1:T}$, prior mean μ_1 and covariance P_1 , initial estimate of β and θ
 - Obtain $\hat{\theta}$ from (21) initialised at β and θ

Importantly, parameterising each joint distribution using the Cholesky factor, $P_k^{\frac{1}{2}}$, allows the components of $I_2(\beta, \theta)$ and $I_3(\beta, \theta)$ corresponding to each time step to be easily approximated using Gaussian quadrature as

$$\hat{I}_{2_k}(\beta_k, \theta) = \sum_{j=1}^{n_s} w_j \log p_{\theta}(x_{k+1}^j | x_k^j), \quad (19a)$$

$$\hat{I}_{3_k}(\beta_k, \theta) = \sum_{j=1}^{n_s} w_j \log p_{\theta}(y_k | x_k^j), \quad (19b)$$

where w_j is a weight, and the n_s sigma points are denoted as $\bar{x}^j \in \mathcal{R}^{2n_x \times 1}$ where $\bar{x}^j = [(x_k^j)^{\top}, (x_{k+1}^j)^{\top}]^{\top}$ is given by linear combinations of the joint mean $[\mu_k^{\top}, \bar{\mu}_k^{\top}]^{\top}$ and the columns of $P_k^{\frac{1}{2}}$. The sigma points, \bar{x}^j , being linear combinations of the elements of β_k is critical as it significantly simplifies the calculation of both first- and second-order derivatives used in the optimisation. This allows $\mathcal{L}(\beta, \theta)$ to be, tractably, approximated by $\hat{\mathcal{L}}(\beta, \theta)$ as

$$\hat{\mathcal{L}}(\beta, \theta) = I_1(\beta) + \hat{I}_2(\beta, \theta) + \hat{I}_3(\beta, \theta) - I_4(\beta), \quad (20)$$

under the assumption of a Gaussian prior where $I_1(\beta)$, $\hat{I}_2(\beta, \theta)$, $\hat{I}_3(\beta, \theta)$, and $I_4(\beta)$ are detailed in Appendix A.

This selected parametrisation is, however, over-parameterised as the marginal distribution $q_{\beta}(x_k)$ can be calculated from either $q_{\beta}(x_{k-1}, x_k)$ or $q_{\beta}(x_k, x_{k+1})$. The nonlinear constraints defined by the feasible set

$$\Omega := \{\beta \in \mathcal{R}^{n_{\beta}} \mid c_k(\beta) = 0, \quad k = 1, \dots, T-1\},$$

where $n_{\beta} = T(2n_x + n_x(2n_x + 1))$ and

$$c_k(\beta) = \left[\text{vech}(B_k^{\top} B_k + C_k^{\top} C_k) - \text{vech}(A_{k+1}^{\top} A_{k+1}) \right],$$

are therefore required to ensure consistency. Here, $\text{vech}(X)$ stacks distinct elements of the symmetric matrix X [15].

This results in a tractable optimisation problem given by

$$\hat{\beta}, \hat{\theta} = \arg \max_{\beta, \theta} \hat{\mathcal{L}}(\beta, \theta), \quad (21a)$$

$$\text{s.t. } \beta \in \Omega, \quad (21b)$$

where $\hat{\theta}$ is the estimated parameter vector. This constrained optimisation problem is of standard form and it can be solved using exact first- and second-order derivatives without any further approximations to a local maximum. The resulting approach to system identification is summarised in Algorithm 1.

The constrained formulation of the optimisation problem differs from the approach usually taken in VI, where unconstrained formulations are typically used. In order to decouple each joint distribution, and to significantly simplify the calculation of second-order derivatives, the resulting optimisation problem has been over-parameterised; nonlinear constraints are introduced to maintain equivalence to the original problem. This over-parametrisation and introduction of constraints to reduce the complexity of the optimisation differs from typical VI approaches. Indeed one of the most common approaches in VI [3] is to assume a *mean-field variational family* [2], or decoupled, assumption in the form of $q_{\beta}(\mathbf{x})$ to similarly simplify calculations. In the context of state space models, this corresponds to assuming mutual independence between consecutive time steps, or even individual states, a clearly inappropriate assumption for state-space models. In contrast the proposed, constrained, approach allows for simplification of the optimisation problem without the introduction of avoidable, and undesirable, assumptions.

3.3 Additive Gaussian Noise

In this section we consider a simplification that can be used for nonlinear systems with additive Gaussian noise. This enables a reduction in the number of optimisation variables, brings numerical benefits, and enables an effective approximation of the Hessian to be formed utilising only first-order derivatives.

We consider a model structure of the form

$$x_{k+1} = f(x_k, \phi) + q_k, \quad (22a)$$

$$y_k = h(x_k, \phi) + r_k, \quad (22b)$$

where $q_k \sim \mathcal{N}(0, Q)$, $r_k \sim \mathcal{N}(0, R)$, and $\theta = \{\phi, Q, R\}$ includes model parameters ϕ , process noise parameters Q , and measurement noise parameters R .

While independence of q_k and r_k has been assumed, in many practical situations this may be unwarranted [40] and the consideration of cross correlated noise given by

$$\begin{bmatrix} q_k \\ r_k \end{bmatrix} = \mathcal{N} \left(\begin{bmatrix} 0 \\ 0 \end{bmatrix}, \begin{bmatrix} Q & S \\ S^\top & R \end{bmatrix} \right) \quad (23a)$$

$$= \mathcal{N}(0, \Pi), \quad (23b)$$

may be desired. Using the proposed method this is achieved by not separating $\hat{I}_2(\beta, \theta)$ and $\hat{I}_3(\beta, \theta)$ without further modifications for either the general form, Algorithm 1, or the additive Gaussian noise specialisation of the proposed method considered here. Coupled noise is considered in the numerical examples for both forms of the proposed approach. However, for clarity, only the equations relating to uncorrelated noise are presented.

Using (19) and (22), we can evaluate $\hat{I}_2(\beta, \theta)$ and $\hat{I}_3(\beta, \theta)$ as

$$\hat{I}_2(\beta, \theta) = -\frac{T}{2} \log |2\pi Q| - \frac{1}{2} \sum_{k=1}^T \sum_{j=1}^{n_s} w_j \left\| \xi_k^j \right\|_{Q^{-1}}^2, \quad (24a)$$

$$\hat{I}_3(\beta, \theta) = -\frac{T}{2} \log |2\pi R| - \frac{1}{2} \sum_{k=1}^T \sum_{j=1}^{n_s} w_j \left\| \varepsilon_k^j \right\|_{R^{-1}}^2, \quad (24b)$$

where

$$\xi_k^j = x_{k+1}^j - f(x_k^j, \phi), \quad \varepsilon_k^j = y_k - h(x_k^j, \phi), \quad (25)$$

and (x_k^j, x_{k+1}^j) are sigma points from the joint normal distribution $q_{\beta_k}(x_k, x_{k+1})$.

A result of the structure arising from the additive Gaussian assumption is the optimal Q^* and R^* satisfy

$$Q^*(\phi, \beta) = \frac{1}{T} \bar{x} \bar{x}^\top, \quad R^*(\phi, \beta) = \frac{1}{T} \bar{y} \bar{y}^\top, \quad (26)$$

where

$$\begin{aligned} \bar{x} &= [\bar{x}_1, \dots, \bar{x}_T], & \bar{x}_k &= [\sqrt{w_1} \xi_k^1, \dots, \sqrt{w_{n_s}} \xi_k^{n_s}], \\ \bar{y} &= [\bar{y}_1, \dots, \bar{y}_T], & \bar{y}_k &= [\sqrt{w_1} \varepsilon_k^1, \dots, \sqrt{w_{n_s}} \varepsilon_k^{n_s}]. \end{aligned}$$

This property is also used for in the M-step of approximate EM methods [20, 35].

Substituting (26) into (24a) and (24b) yields

$$I_2^{\text{D}}(\phi, \beta) = c_2 - \frac{T}{2} \log |Q^*(\phi, \beta)|, \quad (27a)$$

$$I_3^{\text{D}}(\phi, \beta) = c_3 - \frac{T}{2} \log |R^*(\phi, \beta)|, \quad (27b)$$

respectively, where c_2 and c_3 are constants that do not depend on ϕ or β . Thus, we can pose the reduced problem,

$$\hat{\beta}, \hat{\phi} = \arg \max_{\phi, \beta} \hat{\mathcal{L}}_{\text{ID}}(\phi, \beta), \quad (28a)$$

$$\text{s.t. } \beta \in \Omega, \quad (28b)$$

Algorithm 2 Additive Gaussian noise specialisation

Input: Measurements $y_{1:T}$, prior mean μ_1 and covariance P_1 , initial estimate of β and ϕ

- Obtain $\hat{\phi}$ from (28) initialised at β and ϕ
 - Obtain Q and R from (26)
-

where $\hat{\mathcal{L}}_{\text{ID}}(\phi, \beta) = I_1(\beta) + I_2^{\text{ID}}(\phi, \beta) + I_3^{\text{ID}}(\phi, \beta) - I_4(\beta)$. Estimates of Q and R are obtained by evaluating $Q^*(\phi^*, \beta^*)$ and $R^*(\phi^*, \beta^*)$, respectively. The resulting specialisation of the proposed approach to system identification is summarised in Algorithm 2.

Compared with the general formulation, which could be used, this specialisation possesses several benefits. Firstly, the number of variables required to be optimised is reduced while still addressing the original underlying problem. Secondly, using only the Jacobian of $f(x_k, \phi)$ and $h(x_k, \phi)$, the exact gradient, and a good Hessian approximation, of $\hat{\mathcal{L}}_{\text{ID}}(\phi, \beta)$, can be obtained; this is discussed further in Section 4.3 which focuses on the resulting optimisation problem.

4 Implementation

In this section several key points regarding implementation details and the resulting optimisation problems are considered. Section 4.1 briefly examines the Gaussian quadrature used for the integral approximations, Section 4.2 examines the initialisation of the resultant optimisation problems, and Section 4.3 provides some details regarding the optimisations required.

4.1 Gaussian Quadrature

In the numerical examples, a third-order unscented transform [18, 39] with $\alpha = 1$, $\kappa = 0$, and $\beta = 0$ has been used for all Gaussian quadrature approximations. Higher-order methods, such as those detailed in [20], can alternatively be used at a higher computational cost.

4.2 Initialisation

Similar to all identification approaches for nonlinear systems an initial estimate of θ must be provided and influences both the run-time required, and potentially, the parameter estimate produced. Compared to EM-based approaches, however, to utilise the proposed approach an initial estimate of each pairwise joint distribution must also be provided. This is an advantage of the proposed approach as it introduces an added level of flexibility that may be exploited. This added freedom, however, is not required to be utilised; similar to EM approaches an assumed Gaussian smoother could be used to provide this initialisation.

Alternatively, other methods can be used to initialise the state distributions, this initialisation does not need to satisfy the constraints. Generally, it has been found that using the distributions from a filtering pass has proven both an effective and straightforward initialisation. The initial state distribution can also be selected using problem-specific knowledge, examples of this include where estimates of the states can be simply calculated from the measurements. This is particularly beneficial for the additive noise specialisation (Section 3.3) as it removes the requirement to provide initial estimates for Q and R which, generally, are not initially well known.

Due to the general nonlinear nature of the optimisation problems, no concrete method describing the 'best' initialisation scheme, or how to ensure undesirable local minima are encountered is possible. There also exists a general belief that gradient-based searches within system identification present significant problem regarding many undesired local minima and are overly sensitive to the parameter initialisation [36, 25, 24, 31]. In light of these points, the numerical examples in Section 5 are heavily focused on the robustness of the proposed method with respect to initialisation of the parameters and utilise all the approaches to initialising the state distributions discussed.

4.3 Optimisation

As stated, the resulting optimisation problems are of standard form and can be solved using standard solvers. In the numeric examples, the solvers `fmincon` [28] and `KNITRO` [4] are both used. The finer details of the optimisation routines are well beyond the scope of this paper; further details can be found in [28, 4, 32, 7]. In this section, we briefly examine calculation of the required first- and second-order derivatives to highlight the fact that these can be readily obtained with a linear in time computational complexity with respect to the number of measurements.

To perform the optimisation effectively exact first- and second order are used when performing the general form of the proposed approach given in Algorithm 1. Due to the assumed Gaussian distributions closed form expressions exist for $I_1(\beta)$, $I_4(\beta)$, and both the constraint Jacobian and related components of the Hessian; these expressions can be found using matrix calculus [27]. The terms $\hat{I}_2(\beta, \theta)$ and $\hat{I}_3(\beta, \theta)$, however, are general nonlinear functions and do not possess closed forms. Due to the careful parametrisation of the optimisation problem, to ensure that each sigma point is a linear combination of the variables, exact gradients and an exact Hessian can be efficiently obtained automatically. This is achieved using automatic differentiation [14], for which many tools exist; we have used CasADi [1]. By further introducing a copy of θ for each time step, denoted θ_k , and the constraints $\theta_1 = \theta_2 = \dots = \theta_T$, this results in a sparse block diagonal Hessian. As such, the Hessian can be both formed and decomposed within the optimisation routine with a linear in time computational complexity with respect to the number of measurements.

For the additive noise specialised the derivatives for $I_2^{\text{ID}}(\phi, \beta)$ and $I_3^{\text{ID}}(\phi, \beta)$ are calculated differently. Using the matrix calculus exact gradients can be found using only the Jacobian of $f(x_k, \phi)$ and $h(x_k, \phi)$. The Hessian of $I_2^{\text{ID}}(\phi, \beta)$, $I_3^{\text{ID}}(\phi, \beta)$, or the combined form used when coupled noise terms are considered, are all of the form

$$H_{23} = J_n^T J_n - V^T V + S, \quad (29)$$

where $J_n^T J_n$ and $V^T V$ both only require the model Jacobian to obtain and S contains second-order terms. The Hessian is approximated as

$$H_{23} \approx J_n^T J_n - V^T V, \quad (30)$$

where $J_n^T J_n$ is block diagonal and $V^T V$ is dense, where $V \in \mathcal{R}^{(n_x+n_y)^2 \times T n_b}$ and n_b is the dimension of the diagonal blocks. For large T this renders both calculation, and subsequent decomposition's, involving H_{23} intractable. This Hessian approximation can, however, tractably be used within optimisation routines such as `fmincon` and `KNITRO` which accept Hessian-vector multiplications and avoid explicitly forming $V^T V$.

Alternatively, we have developed a custom trust region optimisation routine which can fully utilise this Hessian approximation via a factorisation. Full details of the custom solver developed are beyond the scope of this paper and is based upon the approaches in [32, 7, 29].

Central to the optimisation process are solutions of the KKT system of the form

$$\begin{bmatrix} \bar{H} - V^T V & A^T \\ A & 0 \end{bmatrix} \begin{bmatrix} \eta \\ \lambda \end{bmatrix} = - \begin{bmatrix} r_1 \\ r_2 \end{bmatrix}, \quad (31)$$

where A is the sparse constraint Jacobian, r_1, r_2 are vectors, and \bar{H} represents all the block diagonal components of the Hessian. This is intractable due to the dense term $V^T V$. Solutions of this system are, alternatively, obtained by solving the tractable augmented system

$$\begin{bmatrix} \bar{H} & A^T & V^T \\ A & 0 & 0 \\ V & 0 & I \end{bmatrix} \begin{bmatrix} \eta \\ \lambda \\ \gamma \end{bmatrix} = - \begin{bmatrix} r_1 \\ r_2 \\ 0 \end{bmatrix}. \quad (32)$$

While this system can be handled by sparse linear solvers, in the custom solver developed this system is solved in a structure exploiting fashion which directly operates on the dense blocks. This is achieved by rearranging the system corresponding to interleaving r_1 and r_2 , resulting in an augmented block tri-diagonal system which is efficiently solved. This represents the most computationally costly step of the overall identification process.

5 Examples

In this section, we present four numerical examples where the proposed identification approach is profiled; a linear system (Section 5.1), a stochastic volatility model (Section 5.2), a simple robotic system (Section 5.3), and an inverted pendulum using real data (Section 5.4).

For all examples, unless specified otherwise, the proposed approach refers to the general form of the identification given by Algorithm 1.

5.1 Linear System

Let us consider the linear system

$$H(s) = \frac{0.101}{s^4 + 0.06s^3 + 1.011s^2 + 0.02041s + 0.0101}.$$

The linearity of the system has two important consequences when considering the proposed approach. Firstly, the form of assumed density matches the true distribution, and secondly, the Gaussian quadrature used exactly calculates the required integrals.

Measurements from 100 samples of a 0.5 s discretisation with $Q = \text{diag}(10, 10, 100, 1000)$, $R = 0.1$ are used to estimate A , B , C , D , and Π . The proposed method, limited to 1×10^3 iterations, is compared against 50×10^3 iterations of the linear EM method detailed in [12]. A state prior of $\mathcal{N}(0, I)$ and model parameters initialised using a subspace method [23] is used for both approaches. The state distributions for the proposed approach were initialised using the corresponding smoothed states.

Figure 1 shows the log-likelihood at each iteration for both methods. This results shows that, as expected, both methods have produced similar results and the proposed method has an improved rate of convergence over EM.

In this section, we have demonstrated that the proposed approach performs satisfactorily on linear systems. As linear systems inherently satisfy the assumptions of the approach, the closely matching results to linear EM serves as a verification of the implementation.

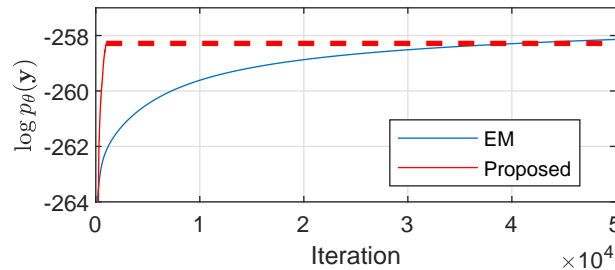


Figure 1: Log-likelihood for each iteration for EM (blue) and the proposed (red) method. The line for proposed method is extended (red dashed) past the 1000-iteration limit for clarity.

5.2 Stochastic Volatility Model

In this example we consider the estimation of $\theta = [a, b, c]$ for the following stochastic volatility model

$$x_{k+1} = a + bx_k + \sqrt{c}w_k, \quad (33a)$$

$$y_k = \sqrt{e^{x_k}}v_k, \quad (33b)$$

where $w_k \sim \mathcal{N}(0, 1)$ and $v_k \sim \mathcal{N}(0, 1)$. The data consists of daily Bitcoin price data from November 7, 2015, to November 7, 2017, resulting in 726 measurements. Results obtained using CPF-SAEM [22] are used to compare against.

For the proposed method, each joint state distribution is initialised with a mean of $[2, 2]^T$ and a diagonal covariance with standard deviations of 0.1. An initial parameter estimate of $\theta = [0, 0.5, 1]^T$ is used for both approaches, and 50 particles were used for the CPF-SAEM approach.

The proposed method converged in 19 iterations using `fmincon` [28] to perform the optimisation. In contrast, CPF-SAEM did not converge and is limited to 1000 iterations. Figure 2 shows the parameter trajectory of both methods and highlights that similar parameter estimates are obtained. CPF-SAEM, however, requires a significantly larger quantity of iterations and has only approached the parameter values obtained by the proposed method.

The robustness to initial estimates of the proposed method has also been examined using 100 random initial parameter estimates sampled from

$$a \sim \mathcal{U}(-0.5, 0.5), \quad b \sim \mathcal{U}(0, 1.5), \quad c \sim \mathcal{U}(0.25, 2),$$

Parameter trajectories for each trial are plotted in Figure 3 and shows that each initialisation has converged to the same parameter estimate.

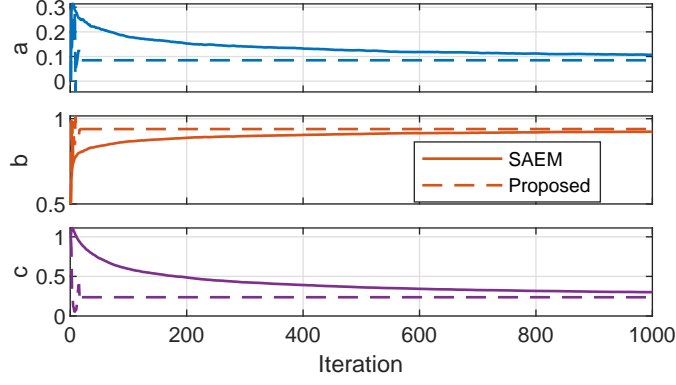


Figure 2: Parameter trajectory vs. iteration count. The lines for the proposed method have been extended beyond 19 iterations for clarity.

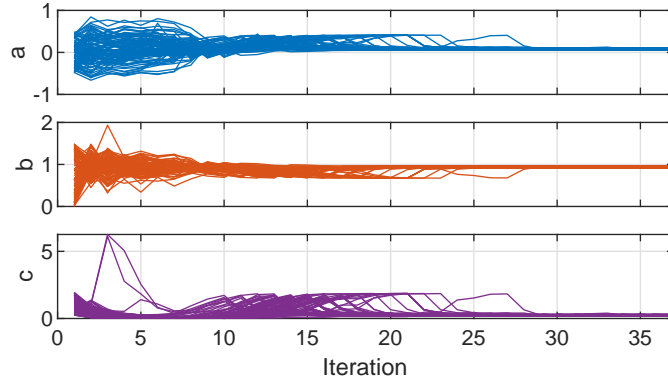


Figure 3: Parameter trajectory vs. iteration count for 100 random initial estimates using the proposed method.

In this section, the proposed system identification approach is applied to a system without additive Gaussian noise and compared favourably with CPF-SAEM. This required no alterations to the proposed approach, which proved to be both effective and robust to initial parameter estimates.

5.3 Robot Model

In this example, we consider a continuous-time model of a two-wheeled robot given by

$$\begin{bmatrix} \dot{q}_1(t) \\ \dot{q}_2(t) \\ \dot{q}_3(t) \\ \dot{p}_1(t) \\ \dot{p}_2(t) \end{bmatrix} = \begin{bmatrix} \frac{\cos(q_3(t))p_1(t)}{m} \\ \frac{\sin(q_3(t))p_1(t)}{m} \\ \frac{p_2(t)}{J+ml^2} \\ \frac{-r_1p_1(t)}{m} - \frac{mlp_2^2(t)}{(J+ml^2)^2} + u_1(t) + u_2(t) \\ \frac{(lp_1(t)-r_2)p_2(t)}{J+ml^2} + au_1(t) - au_2(t) \end{bmatrix}, \quad (34)$$

where $r_1 = 1$, $r_2 = 1$, $a = 0.5$, $m = 5$, $J = 0.2$, $l = 0.15$, $u_1(t)$ is the force applied to the left wheel, $u_2(t)$ is the force applied to the right wheel, and the state vector $x(t) = [\dot{q}_1(t), \dot{q}_2(t), \dot{q}_3(t), \dot{p}_1(t), \dot{p}_2(t)]^\top$ consists of x-position, y-position, heading, linear momentum, and angular momentum states respectively. A 50 s simulated trajectory is generated using an ODE solver disturbed by noise sampled from $\mathcal{N}(0, Q)$ where $Q = \text{diag}(0.001, 0.001, 1.745 \times 10^{-3}, 0.001, 0.001)$ at 0.1 s intervals. Measurements at each interval are obtained according to

$$y_k = [q_1(t), q_2(t), q_3(t)]^\top + e_k, \quad e_k \sim \mathcal{N}(0, R),$$

where $R = \text{diag}(0.1^2, 0.1^2, 0.0349^2)$. This model has been considered in the context of state estimation in [8].

5.3.1 Convergence

In this section, the convergence when estimating m , l , r , and noise terms Q , and R is examined. For the proposed method, the optimisation is performed using KNITRO [4]. The results are compared against two EM approaches

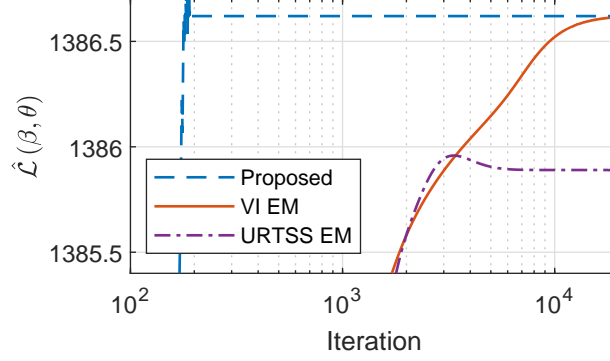


Figure 4: Comparison of proposed, VI-EM, and URTSS-EM approaches to identification on a simulated robot example. Proposed extended past the 194 iterations required for convergence for clarity.

which approximate the smoothing step using the URTSS [34] and the VI smoother in [8]; these are denoted URTSS-EM and VI-EM respectively. From Section 2.2, the VI-EM corresponds to variational EM. As such, VI-EM is expected to converge towards the same values as the proposed method, albeit at a slower rate. For each method an initial parameter estimate of $m = 10$, $J = 4$, $l = 0.3$, and

$$Q = \text{diag} (0.01^2, 0.01^2, 0.0035^2, 0.01^2, 0.01^2),$$

$$R = \text{diag} (0.1^2, 0.1^2, 0.0349^2),$$

was used. The state distributions for the proposed method were initialised using the filtered distributions obtaining using the method of [8]. The proposed method converged to a locally optimal solution in 194 iterations, neither of the EM approaches converged within the 20×10^3 iteration limit. The cost obtained for each method, as a function of iteration count, is shown in Figure 4 and shows the 194 iterations of the proposed method has outperformed the 20×10^3 iterations of both the EM approaches. As expected the VI-EM approach asymptotically approaches the cost achieved by the proposed method. Contrary to this, URTSS-EM does not, neither does it maintain the desired monotonic behaviour of EM. Both of these properties highlight the benefit of following the more principled approach in regards to any approximations introduced.

5.3.2 Robustness to Initialisation

In this section, the robustness of the proposed method to the initial parameter estimate is examined. For this estimation of m , l , r , and coupled noise term Π is considered from 75 differing parameter initialisations given by

$$m \sim \mathcal{U}(0.5, 15), \quad J \sim \mathcal{U}(0.01, 10), \quad l \sim \mathcal{U}(0.01, 0.5),$$

$$Q = \text{diag} (0.1^2, 0.1^2, 0.0349^2, 0.1^2, 0.1^2),$$

$$S = 0_{n_x \times n_y},$$

$$R = \text{diag} (0.5^2, 0.5^2, 0.1745^2).$$

The state distributions for the optimisation were initialised by running the URTSS from the initial parameter estimates.

Table 1 shows a subset of the estimated parameters for this experiment. The third column shows the mean parameter estimate for each of the 75 trials, and is an effective estimate of the true parameters. The fourth column shows the maximum difference between this mean and each individual trials. The small values indicate that each of the 75 trials converged to the same parameter estimate, subject to a small tolerance.

These results indicates the robustness of the proposed approach and highlights that, at least on this example, the proposed method does not suffer from a potentially large quantity of undesirable local minima. The estimates for Π performed similarly as the parameters shown in Table 1, but due to its multi-variable nature the numerical values are not included for brevity.

5.4 Inverted Pendulum System

In this section identification of a rotational inverted pendulum, or Furata pendulum [10], is considered using real data collected from a Quanser QUBE - Servo 2. This system consists of a driven horizontal rod attached to a

Table 1: Parameter estimate for 75 differing initial parameter estimates to illustrate robustness.

Parameter	True	Estimated	Maximum difference
m	5	5.07	6.39×10^{-6}
J	2	2.24	4.98×10^{-6}
l	0.15	0.14	7.48×10^{-7}

pendulum which spins freely in the vertical plane and provides measurements of rod angle, pendulum angle, and motor current.

Throughout this section estimation of the rod friction D_r , pendulum friction D_p , rod inertia J_r , pendulum inertia J_p , motor constant k_m , motor resistance R_m , and coupled additive noise term Π is considered using the four state, continuous time, model detailed in Appendix B. This is discretised using two-step Euler integration for each 8 ms sample. The modelling assumption of coupled additive Gaussian noise for the process and measurement models is also applied. The important property of the first-principle model utilised is the presence of many nonlinearities for both state and parameter variables.

5.4.1 Robustness to Initialisation

The effectiveness and robustness of the additive noise specialisation of the proposed method (Algorithm 2) is compared against CPF-SAEM from 50 differing parameter initialisations sampled from

$$\begin{aligned}
 J_r &\sim \mathcal{U}(1 \times 10^{-7}, 0.01), & D_r &\sim \mathcal{U}(1 \times 10^{-7}, 0.01), \\
 J_p &\sim \mathcal{U}(1 \times 10^{-7}, 0.01), & D_p &\sim \mathcal{U}(1 \times 10^{-7}, 0.01), \\
 k_m &\sim \mathcal{U}(0.001, 1), & R_m &\sim \mathcal{U}(4, 15),
 \end{aligned}$$

with the noise covariance terms initialised as

$$\begin{aligned}
 Q &= \text{diag} (7.6154 \times 10^{-5}, 7.6154 \times 10^{-5}, 0.0012, 0.0012), \\
 S &= 0_{n_x \times n_y}, \\
 R &= \text{diag} (3.0462 \times 10^{-4}, 3.0462 \times 10^{-4}, 0.01),
 \end{aligned}$$

on a single data set consisting of 375 measurements during which the pendulum undergoes full rotations. Note that the noise terms are only utilised for the CPF-SAEM approach, as per Section 4.2 they are not required for the additive noise version of the proposed approach.

For each of these trials, the state distributions were initialised with a mean of corresponding to the measurements for the position states with a 1° standard deviation and a mean for the velocity states corresponding to a finite difference of the position measurements with a standard deviation of 10°s^{-1} . A relative function tolerance of 1×10^{-8} on $\hat{\mathcal{L}}_{\text{ID}}(\phi, \beta)$ was used as a termination condition. This required a median of 170 iterations and 112 s to complete. Importantly, the proposed method proved to be robust with respect to the differing initialisations with all initialisations converging to the same value subject to a small numeric tolerance.

The CPF-SAEM approach was performed using a fully adapted auxiliary particle filter [33] with 100 particles, 50 particles for the backwards simulation smoother [13], and a burn-in of 100 iterations before application of the stochastic approximation. The iterations were terminated when the change in all parameter estimates between successive iterations fell below 1×10^{-3} for 5 of the last 10 iterations. These settings have been selected as a trade-off between performance and run-time and required a median of 156 iterations and 308 s to complete. In contrast to the proposed method, the results using CPF-SAEM were inconsistent and highly dependant upon the selection of particle count, burn-in window, and termination criteria; using the provided settings CPF-SAEM failed on 12 of the 50 trials.

In Table 2 the mean and standard deviation of the estimated parameter values of each successful trial are shown. The closeness of the mean parameter estimates for the proposed method to the successful CPF-SAEM trials illustrates that despite the approximations introduced, similar parameter estimates are obtained; the values obtained are also close to the expected values for this physical system. While not included for clarity the estimation of the noise term Π performed similarly.

These results highlight some important properties of the proposed approach. Firstly, the robustness to the initialisation of the parameters, all differing initialisations have converged to the same parameter estimate, subject to a

Table 2: Mean and standard deviation of the parameter estimates for each successful trial from 50 differing initial values. Twelve of the CPF-SAEM runs were unsuccessful and have been censored.

Parameter	Proposed	CPF-SAEM
J_r	$1.07 \times 10^{-4} \pm 8.17 \times 10^{-11}$	$1.08 \times 10^{-4} \pm 3.27 \times 10^{-7}$
J_p	$2.92 \times 10^{-5} \pm 3.32 \times 10^{-11}$	$2.90 \times 10^{-5} \pm 7.80 \times 10^{-8}$
k_m	$4.57 \times 10^{-2} \pm 2.73 \times 10^{-8}$	$4.99 \times 10^{-2} \pm 4.60 \times 10^{-4}$
R_m	$9.59 \pm 4.06 \times 10^{-7}$	$1.02 \times 10^1 \pm 7.42 \times 10^{-2}$
D_p	$4.68 \times 10^{-5} \pm 7.66 \times 10^{-11}$	$5.03 \times 10^{-5} \pm 7.24 \times 10^{-7}$
D_r	$2.81 \times 10^{-4} \pm 1.87 \times 10^{-9}$	$2.15 \times 10^{-4} \pm 4.32 \times 10^{-6}$

Table 3: Parameter estimates for seven differing data sets.

	J_r	J_p	k_m	R_m	D_p	D_r
Data set 1	1.04×10^{-4}	2.95×10^{-5}	4.54×10^{-2}	9.65	3.16×10^{-5}	4.00×10^{-4}
Data set 2	1.05×10^{-4}	2.92×10^{-5}	4.56×10^{-2}	9.59	2.88×10^{-5}	4.07×10^{-4}
Data set 3	1.70×10^{-4}	2.92×10^{-5}	4.57×10^{-2}	9.59	4.68×10^{-5}	2.81×10^{-4}
Data set 4	1.12×10^{-4}	3.05×10^{-5}	4.75×10^{-2}	9.67	1.61×10^{-5}	2.02×10^{-4}
Data set 5	1.13×10^{-4}	2.95×10^{-5}	4.61×10^{-2}	9.86	2.87×10^{-5}	3.38×10^{-4}
Data set 6	1.10×10^{-4}	3.03×10^{-5}	4.59×10^{-2}	9.58	2.03×10^{-5}	3.90×10^{-4}
Data set 7	1.11×10^{-4}	2.93×10^{-5}	4.50×10^{-2}	9.60	6.13×10^{-6}	3.95×10^{-4}

small numeric tolerance. Secondly, despite the assumed density form, and integral approximation introduced, the resulting parameter estimate are close to those produced by particle methods and require less run-time to converge to a much higher tolerance.

5.4.2 Robustness to Data

In this section, the robustness and consistency of estimated parameters with respect to the data set utilised is examined using seven differing data sets which contain significantly differing state trajectories. For each data-set parameter estimates are initialised using the same five random samples, the state distributions are initialised as previously discussed.

Using the additive noise specialisation of the proposed method (Algorithm 2) all of these trials were successful. The maximum relative standard deviation between the parameters estimated for each data set from the differing initialisations was 1.0062×10^{-4} , again illustrating robustness with respect to parameter initialisation. The focus of the section, however, is the variation in the estimated parameters between the differing data sets. The mean estimated parameters for each data set are given in Table 3 and illustrates that similar values have consistently been obtained.

In this section, the proposed system identification method has been applied to a real unstable system using seven different data sets. The results obtained shows the applicability of the approach to a system of practical interest. The results, furthermore, emphasise the robustness and consistency of the proposed approach with respect to both parameter initialisation and measurement realisation.

6 Conclusion

The contribution of this paper is to present a VI based approach to system identification for nonlinear state-space models. The resulting system identification approach consists of a single, deterministic, optimisation problem. Due to the assumed density and constrained parametrisation chosen, this optimisation problem is of a standard form and is efficiently solved using readily available exact first- and second-order derivatives. A specialisation for systems with additive Gaussian noise was also presented. The proposed method has been numerically examined on a range of simulated and real examples to illustrate the robustness and effectiveness and is compared favourably to state-of-the-art alternatives.

References

- [1] Joel A. E. Andersson, Joris Gillis, Greg Horn, James B. Rawlings, and Moritz Diehl. CasADi: a software framework for nonlinear optimization and optimal control. *Mathematical Programming Computation*,

- 11(1):1–36, July 2018.
- [2] Christopher M. Bishop. *Pattern Recognition and Machine Learning*. Springer-Verlag New York Inc., 2006.
 - [3] D. Blei, A. Kucukelbir, and J. McAuliffe. Variational inference: A review for statisticians. *Journal of the American Statistical Association*, 112(518):859–877, 2017.
 - [4] Richard H. Byrd, Jorge Nocedal, and Richard A. Waltz. Knitro: An Integrated Package for Nonlinear Optimization. In *Nonconvex Optimization and Its Applications*, pages 35–59. Springer US, 2006.
 - [5] Olivier Cappé, Eric Moulines, and Tobias Ryden. *Inference in Hidden Markov Models*. Springer, 2007.
 - [6] S. B. Chitralakha, J. Prakash, H. Raghavan, R. B. Gopaluni, and S. L. Shah. Comparison of Expectation-Maximization based parameter estimation using Particle Filter, Unscented and Extended Kalman Filtering techniques. *IFAC Proceedings Volumes*, 42(10):804–809, 2009.
 - [7] Andrew R. Conn, Nicholas I. M. Gould, and Philippe L. Toint. *Trust Region Methods*. Society for Industrial and Applied Mathematics, January 2000.
 - [8] Jarrad Courts, Adrian Wills, and Thomas B. Schön. Variational Nonlinear State Estimation. *arXiv*, 2020.
 - [9] A. P. Dempster, N. M. Laird, and D. B. Rubin. Maximum likelihood from incomplete data via the EM algorithm. *Journal of the royal statistical society, series B*, 39(1):1–38, 1977.
 - [10] K. Furuta, M. Yamakita, and S. Kobayashi. Swing-up Control of Inverted Pendulum Using Pseudo-State Feedback. *Proceedings of the Institution of Mechanical Engineers, Part I: Journal of Systems and Control Engineering*, 206(4):263–269, November 1992.
 - [11] Matej Gašperin and Dani Juričić. Application of Unscented Transformation in Nonlinear System Identification. *IFAC Proceedings Volumes*, 44(1):4428–4433, January 2011.
 - [12] Stuart Gibson and Brett Ninness. Robust maximum-likelihood estimation of multivariable dynamic systems. *Automatica*, 41(10):1667–1682, October 2005.
 - [13] Simon J. Godsill, Arnaud Doucet, and Mike West. Monte Carlo Smoothing for Nonlinear Time Series. *Journal of the American Statistical Association*, 99(465):156–168, mar 2004.
 - [14] Andreas Griewank and Andrea Walther. *Evaluating Derivatives: Principles and Techniques of Algorithmic Differentiation*. Society for Industrial and Applied Mathematics, jan 2008.
 - [15] Harold V. Henderson and S. R. Searle. Vec and vech operators for matrices, with some uses in jacobians and multivariate statistics. *Canadian Journal of Statistics*, 7(1):65–81, 1979.
 - [16] Rolf Isermann and Marco Münchhof. *Identification of Dynamic Systems*. Springer Berlin Heidelberg, 2011.
 - [17] Michael I. Jordan, Zoubin Ghahramani, Tommi S. Jaakkola, and Lawrence K. Saul. An Introduction to Variational Methods for Graphical Models. *Machine Learning*, 37(2):183–233, November 1999.
 - [18] Simon J. Julier and Jeffrey K. Uhlmann. New extension of the Kalman filter to nonlinear systems. In Ivan Kadar, editor, *Signal Processing, Sensor Fusion, and Target Recognition VI*. SPIE, July 1997.
 - [19] Juho Kokkala, Arno Solin, and Simo Särkkä. Expectation Maximization Based Parameter Estimation by Sigma-Point and Particle Smoothing. In *17th International Conference on Information Fusion (FUSION)*, July 2014.
 - [20] Juho Kokkala, Arno Solin, and Simo Särkkä. Sigma-Point Filtering and Smoothing Based Parameter Estimation in Nonlinear Dynamic Systems. *Journal of Advances in Information Fusion*, 2015.
 - [21] S. Kullback and R. A. Leibler. On Information and Sufficiency. *The Annals of Mathematical Statistics*, 22(1):79–86, March 1951.
 - [22] Fredrik Lindsten. An efficient stochastic approximation EM algorithm using conditional particle filters. In *2013 IEEE International Conference on Acoustics, Speech and Signal Processing*. IEEE, May 2013.
 - [23] L. Ljung. *System Identification: Theory for the User*. Prentice Hall information and system sciences series. Prentice Hall PTR, 1999.
 - [24] L. Ljung. On Convexification of System Identification Criteria. *Automation and Remote Control*, 80(9):1591–1606, September 2019.

- [25] Lennart Ljung. SOME ASPECTS ON NONLINEAR SYSTEM IDENTIFICATION. *IFAC Proceedings Volumes*, 39(1):553–564, 2006.
- [26] Lennart Ljung. Perspectives on system identification. *Annual Reviews in Control*, 34(1):1–12, April 2010.
- [27] Jan R. Magnus and Jan R. Magnus. *Matrix Differential Calculus with Applications in Statistics and Econometrics*. Wiley, February 2019.
- [28] MATLAB. *Optimization Toolbox Release 2018b*. The MathWorks, Inc., Natick, Massachusetts, United States, 2018.
- [29] Jorge J. Moré and D. C. Sorensen. Computing a Trust Region Step. *SIAM Journal on Scientific and Statistical Computing*, 4(3):553–572, September 1983.
- [30] Radford M. Neal and Geoffrey E. Hinton. A View of the EM Algorithm that Justifies Incremental, Sparse, and other Variants. In *Learning in Graphical Models*, pages 355–368. Springer Netherlands, 1998.
- [31] Brett Ninness. Some System Identification Challenges and Approaches. *IFAC Proceedings Volumes*, 42(10):1–20, 2009.
- [32] Jorge Nocedal and Stephen J. Wright. *Numerical Optimization*. Springer New York, second edition, 2006.
- [33] Michael K. Pitt and Neil Shephard. Filtering via Simulation: Auxiliary Particle Filters. *Journal of the American Statistical Association*, 94(446):590–599, June 1999.
- [34] Simo Särkkä. Unscented Rauch–Tung–Striebel Smoother. *IEEE Transactions on Automatic Control*, 53(3):845–849, April 2008.
- [35] Simo Särkkä. *Bayesian Filtering and Smoothing*. Institute of Mathematical Statistics Textbooks. Cambridge University Press, 2013.
- [36] Thomas B. Schön, Adrian Wills, and Brett Ninness. System identification of nonlinear state-space models. *Automatica*, 47(1):39 – 49, 2011.
- [37] Dimitris G. Tzikas, Aristidis C. Likas, and Nikolaos P. Galatsanos. The variational approximation for Bayesian inference. *IEEE Signal Processing Magazine*, 25(6):131–146, November 2008.
- [38] Michail D. Vrettas, Yuan Shen, and Dan Cornford. Derivations of Variational Gaussian Process Approximation Framework. Technical report, Aston University, March 2008.
- [39] E. A. Wan and R. Van Der Merwe. The unscented Kalman filter for nonlinear estimation. In *Proceedings of the IEEE Adaptive Systems for Signal Processing, Communications, and Control Symposium*. IEEE, October 2000.
- [40] Yanhui Wang, Hongbin Zhang, and Yang Li. Iterated posterior linearization filters and smoothers with cross-correlated noises. *ISA Transactions*, 100:264–274, May 2020.

A Calculation of $\hat{\mathcal{L}}(\beta, \theta)$

In this section, the full equations to calculate $\hat{\mathcal{L}}(\beta, \theta)$ are given assuming a Gaussian prior of $\mathcal{N}(x_1; \mu_0, P_0)$.

$$\hat{\mathcal{L}}(\beta, \theta) = I_1(\beta) + \hat{I}_2(\beta, \theta) + \hat{I}_3(\beta, \theta) - I_4(\beta),$$

where

$$\begin{aligned}
I_1(\beta) &= -\frac{n_x}{2} \log 2\pi - \sum_{i=1}^{n_x} \log P_0^{\frac{1}{2}}(i, i) - \frac{1}{2} \text{tr} (P_0^{-1} A_1^T A_1) \\
&\quad - \frac{1}{2} \left(P_0^{-\frac{1}{2}} (\mu_0 - \mu_1) \right)^T \left(P_0^{-\frac{1}{2}} (\mu_0 - \mu_1) \right), \\
\hat{I}_2(\beta, \theta) &= \sum_{k=1}^T \sum_{j=1}^{n_s} w_j \log p_\theta(x_{k+1}^j | x_k^j), \\
\hat{I}_3(\beta, \theta) &= \sum_{k=1}^T \sum_{j=1}^{n_s} w_j \log p_\theta(y_k | x_k^j), \\
I_4(\beta) &= -\frac{(T+1)n_x}{2} \log 2\pi - \frac{(T+1)n_x}{2} \\
&\quad - \sum_{k=1}^T \sum_{i=1}^{n_x} \log C_k(i, i) - \sum_{i=1}^{n_x} \log A_1(i, i).
\end{aligned}$$

Here, the notation $X(i, i)$ refers to the i^{th} diagonal element of X .

B Furata Pendulum Model

The state vector used to model the Furata pendulum is $x = [\vartheta \quad \alpha \quad \dot{\vartheta} \quad \dot{\alpha}]^T$, where ϑ and α are the arm and pendulum angles, respectively.

The continuous time dynamics are given by,

$$\dot{x} = [\dot{\vartheta} \quad \dot{\alpha} \quad \ddot{\vartheta} \quad \ddot{\alpha}]^T,$$

where

$$\begin{aligned}
\begin{bmatrix} \ddot{\vartheta} \\ \ddot{\alpha} \end{bmatrix} &= M^{-1} \left(\begin{bmatrix} \tau - D_r \dot{\vartheta} \\ -D_p \dot{\alpha} - \frac{1}{2} m_p l_p g \sin(\alpha) \end{bmatrix} - C \right), \\
C &= \begin{bmatrix} \frac{1}{2} m_p l_p^2 \sin(\alpha) \cos(\alpha) \dot{\vartheta} \dot{\alpha} - \frac{1}{2} m_p l_p l_r \sin(\alpha) \dot{\alpha}^2 \\ -\frac{1}{4} m_p l_p^2 \cos(\alpha) \sin(\alpha) \dot{\vartheta}^2 \end{bmatrix}, \\
\tau &= \frac{k_m (V_m - k_m \dot{\vartheta})}{R_m}, \\
M &= \begin{bmatrix} M_{11} & M_{12} \\ M_{21} & M_{22} \end{bmatrix}, \\
M_{11} &= J_r + m_p l_r^2 + \frac{1}{4} (m_p l_p^2 - m_p l_p^2 \cos^2(\alpha)), \\
M_{12} &= M_{21} \\
&= \frac{1}{2} m_p l_p l_r \cos^2(\alpha), \\
M_{22} &= J_p + \frac{1}{4} m_p l_p^2,
\end{aligned}$$

and m_p is the pendulum mass, l_r , l_p and the rod and pendulum lengths respectively, J_r , J_p are the rod and pendulum inertias, R_m is the motor resistance, k_m is the motor constant, D_r , D_p are damping coefficients for the rod and pendulum respectively, and V_m is the applied motor voltage input.

The considered process model is a two-step Euler discretisation of these continuous time dynamics over an 8 ms sampling time subsequently disturbed by noise v_k .

Measurements are from encoders on the arm and pendulum angle and current measurement from the motor. The resulting measurement model is

$$y_k = \begin{bmatrix} \vartheta & \alpha & \frac{V_m - k_m \dot{\vartheta}}{R_m} \end{bmatrix}^T + w_k,$$

and it is assumed that

$$\begin{bmatrix} v_k \\ w_k \end{bmatrix} \sim \mathcal{N}(0, \Pi).$$